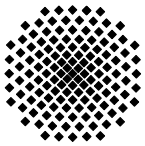

Universität Stuttgart

Performance of IGI AEROcontrol-IId GPS/Inertial System

Final Report

Institute for Photogrammetry (ifp)
University of Stuttgart
Geschwister-Scholl-Str. 24 D
D - 70174 Stuttgart / Germany

Final Report

Performance of IGI AEROcontrol-IId GPS/Inertial System

Institute for Photogrammetry
University of Stuttgart
Geschwister-Scholl-Str. 24 D
D - 70174 Stuttgart / Germany

CONTENTS 1

Introduction

Testing the accuracy performance of a high-end integrated GPS/inertial systems in high dynamic airborne environments is not an easy task, since independent references for the exterior orientations are necessary for the quality checks. One possibility in airborne applications is combining the system with an imaging sensor like a standard photogrammetric camera and flying over a well prepared photogrammetric test site, where the classical indirect method of AT is used to determine independent values for the comparisons. Applying this method for the accuracy tests two things have to be taken into account:

1. As it is well known from theory, the exterior orientations from AT are optimal only in the sense of object point reconstruction. Since they are determined indirectly via an adjustment and only estimated values they are affected by any uncorrected systematic errors and might be different from the physical orientation parameters. On the other hand GPS/inertial systems provide true physical orientation parameters

2. The theoretical accuracy of the orientation parameters from AT is dependent on the image block geometry and the image scale (for positioning information of the camera perspective centre).

Using the results from AT as independent reference the accuracy should be preferable 5-10 times better than the expected accuracy from GPS/inertial. This cannot be guaranteed for high-end integrated systems where the accuracy potential is in the range of 10cm for positioning and 0.003-0.005deg for the attitudes. Therefore, the analysis of the differences at the camera air stations is interpreted as first estimation of the accuracy potential from GPS/inertial only, the overall performance is obtained from re-determined object points using direct georeferencing and the comparison to their given reference coordinates.

Test flight design

For this project the ifp test field Vaihingen/Enz about 25km north-west of Stuttgart/Germany was prepared for the accuracy investigations. This test site covers an area of about 30km² with more than 80 signalized points determined from static GPS surveys and standard photogrammetric AT (Figure 1). Since the accuracy of these object points is about 5cm and better, they are used as references for the overall system accuracy check. The location of the reference points is optimized for two different image flights with different flying height and image scale. The medium scale flight covers the whole test site and is flown in cross-pattern at a flying height of 2000m above ground. During the three long (east-west) and three cross (north-south) strips altogether 36 images are captured. The large image scale block is flown in the eastern part of the area and consists of two north-south strips (~h_g=1000m) only, providing 16 independent values for camera air stations. Since a photogrammetric wide-angle camera was used for the flight mission the different flying heights result in image scales of 1:13000 and 1:6500, respectively.

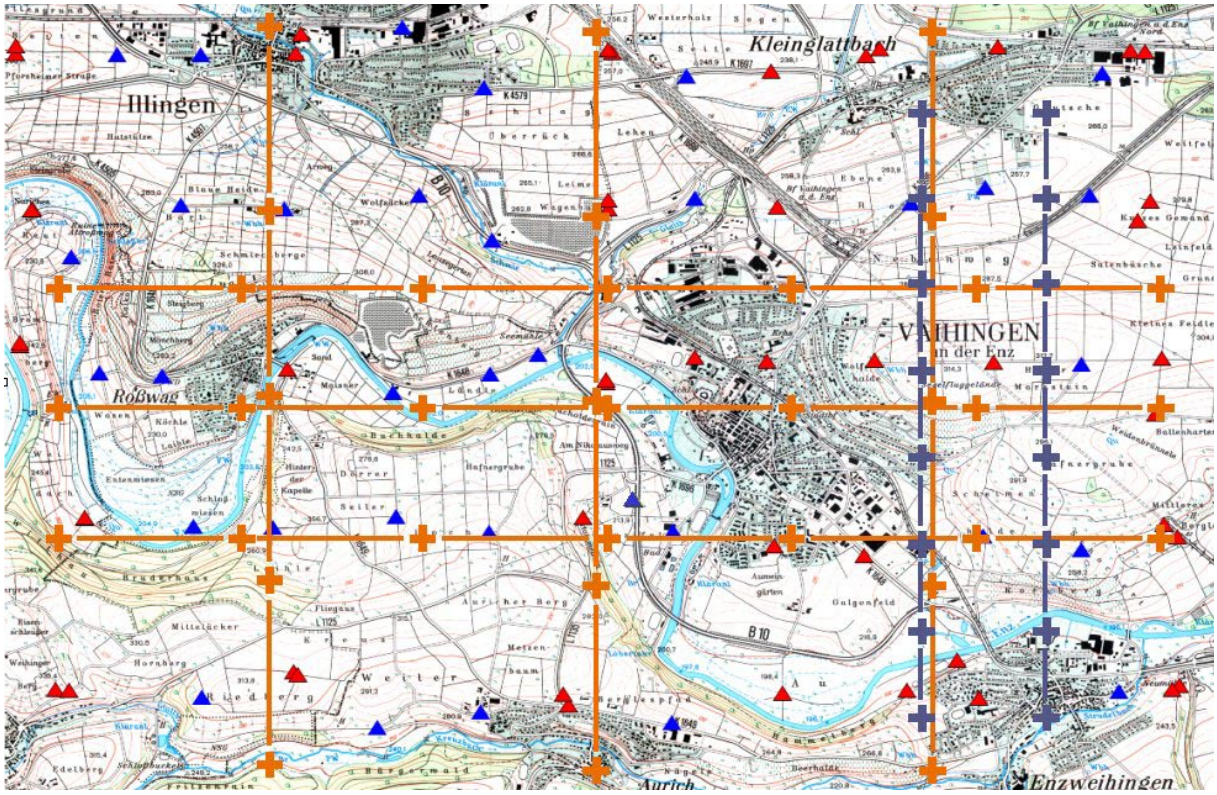

Figure 1, ifp test site Vaihingen/Enz with ground control points and standard flight lines at scale 1:13000 (brown) and 1:6500 (blue) superimposed

To enlarge flying time and number of images the large and medium scale blocks were flown several times. The flight was done by Hansa Luftbild at June 5th, 2000. The corresponding flight trajectory is depicted in Figure 2. Within this mission the 1:13000 scale block was flown three times (108 images, Mission A, Mission B, Mission C) followed by the large scale block (16 images, Mission D), resulting in about 2h photo flight and 124 recorded images. A short static alignment on the runway was performed before starting the mission at an airport about 60km away from the test area. Even advised in mission planning no in-air alignment flight manoeuvre was done before entering the test area. This results in some accuracy problems during the first two flight lines as it will be shown in more details later.

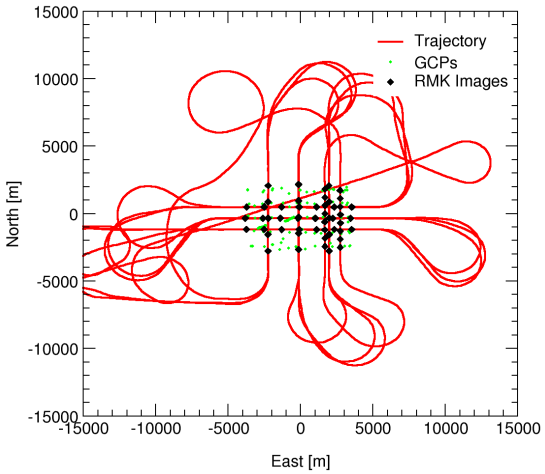

Figure 2, Flight trajectory (June 5th, 2000)

Estimation of reference trajectory from AT

Using the traditional method of AT the recorded photogrammetric images are orientated providing independent values for the exterior orientation elements. Since the estimated values for position and orientation of the camera station from AT are highly correlated as mentioned before – for example a sensor motion in flight direction can be compensated by a different pitch angle –, two different AT versions are calculated for the quality comparisons:

1. The first AT is based only on the ground control points and is used to check the performance of GPS/inertial positioning. The is the standard case of aerial triangulation.

2. For the GPS/inertial attitude accuracy investigation a second AT is necessary, where the ground control points and additionally the GPS/inertial positions are introduced as absolute observations of the camera stations to de-correlate the influence of position and attitude. This corresponds to a GPS-supported AT, where the position observations are used as absolute values without any additional drift parameters.

The two different AT approaches are calculated for each image scale separately. In case of the medium scale blocks (Mission A, B, C) the image coordinates of signalized points were measured manually using the Zeiss PK1 mono-comparator. In case of the large scale images an automatic aerial triangulation was applied. The final bundle adjustment was done using the PATB bundle adjustment software. From inversion of the normal equations the theoretical accuracy of orientation elements from AT is obtained like follows:

Theoretical accuracy of camera perspective centre coordinates from AT (version 1):

Imagery	Mean Std.Dev. σ [m]			Maximum Std.Dev. [m]		
	X_0	Y_0	Z_0	X_0	Y_0	Z_0
1:13000, Mission A,B,C	0.064	0.064	0.029	0.132	0.110	0.067
1:6500, Mission D	0.028	0.023	0.018	0.037	0.038	0.028

Theoretical accuracy of camera orientation angles from AT (version 2):

Imagery	Mean Std.Dev. σ [deg]			Maximum Std.Dev. [deg]		
	ω	φ	κ	ω	φ	κ
1:13000, Mission A,B,C	0.001071	0.001062	0.000645	0.001371	0.001447	0.001059
1:6500, Mission D	0.001515	0.001666	0.000980	0.001991	0.002754	0.001632

Additionally, in Figures 3 and 4 the theoretical accuracy values for the 1:13000 images are depicted for each image separately. The figures show the typical theoretical error behaviour of AT where the accuracy in vertical and kappa-angle is about a factor of two better compared to the horizontal positions and omega- and phi-angle. Since the positioning accuracy is scale dependent the estimated accuracy for the large scale imagery is higher compared to the medium scale images.

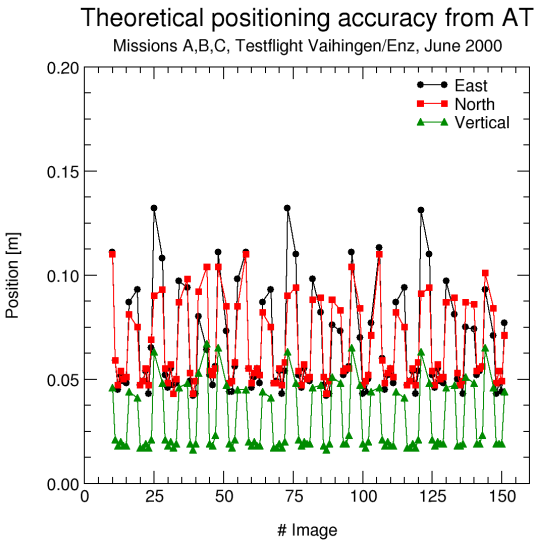

Figure 3, Estimated positioning accuracy from AT

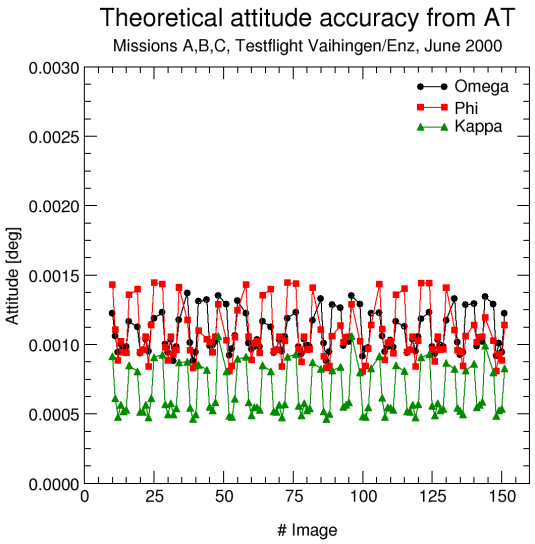

Figure 4, Estimated attitude accuracy from AT

This theoretical accuracy has to be kept in mind when analyzing the differences between exterior orientation from AT and GPS/inertial. Nevertheless, to repeat: The numbers given above did not really reflect the correctness of the estimated exterior orientations from a physical point of view, since they are estimated only and affected by any uncorrected systematic errors and therefore might be significantly different from the true physical image orientation.

Finally, AT and all accuracy investigations were done in a local cartesian topocentric coordinate frame related to the WGS84 ellipsoid in order to avoid errors from coordinate transformations and especially from datum shift.

Performance of orientation elements from IGI AEROcontrol system

AEROoffice software version 3.18, GPS software GrafNav version 6.0 (Waypoint Consulting, Canada)
Exterior orientation elements provided from IGI at 17.01.2001

General remarks

- The processing/integration of GPS/inertial data was completely done by the system manufacturer IGI company. For the accuracy investigations IGI provided the GPS/inertial positions and attitudes interpolated on the camera exposure times.

- The estimation of the boresight angles was done by IGI. For boresight calibration ifp provided the exterior orientations from AT for 9 flight lines altogether. In detail, the boresight was calibrated from 2 flight lines Mission A (lines #5, #6, 10 images), 6 flight lines Mission B (lines #1-#6, 36 images) and 1 flight line Mission C (line #1, 7 images).

- The final system performance presented in the following was obtained in an "iterative process". IGI used the independent data from AT to detect errors or inconsistencies (time delays) in their processing chain. Therefore the reconfirmation of these results using different and independent data sets is mandatory. Additionally, the GPS/inertial processing has to be verified by "normal" users.

Positioning accuracy from 1:13000 imagery

- Differences at camera air stations obtained from 3 x 36 images (Mission A, B, C, 1:13000)

  Statistical analysis [m]

Observation	RMS	Max.Dev.	at Image
East	1.14e-001	4.54e-001	76
North	8.93e-002	3.07e-001	47
Vertical	6.04e-002	2.12e-001	137
Observation	Mean	Std.Dev.	
East	4.60e-002	1.04e-001	
North	-2.55e-004	8.93e-002	
Vertical	-2.89e-002	5.30e-002	

- Differences at camera air stations obtained from 36 images (Mission A, 1:13000)
  Figure 5 Mission A

  Statistical analysis [m]

Observation	RMS	Max.Dev.	at Image
East	1.11e-001	3.62e-001	10
North	8.78e-002	3.07e-001	47
Vertical	6.27e-002	1.93e-001	10
Observation	Mean	Std.Dev.	
East	1.41e-002	1.10e-001	
North	3.23e-002	8.16e-002	
Vertical	-3.86e-002	4.94e-002	

- Differences at camera air stations obtained from 36 images (Mission B, 1:13000)
  Figure 6 Mission B

  Statistical analysis [m]

Observation	RMS	Max.Dev.	at Image
East	1.26e-001	4.54e-001	76
North	8.40e-002	2.17e-001	89
Vertical	5.76e-002	1.68e-001	89
Observation	Mean	Std.Dev.	
East	6.41e-002	1.08e-001	
North	-1.50e-002	8.26e-002	
Vertical	-1.34e-002	5.60e-002	

- Differences at camera air stations obtained from 36 images (Mission C, 1:13000)
  Figure 7 Mission C

  Statistical analysis [m]

Observation	RMS	Max.Dev.	at Image
East	1.05e-001	2.29e-001	124
North	9.57e-002	2.98e-001	137
Vertical	6.07e-002	2.12e-001	137
Observation	Mean	Std.Dev.	
East	5.97e-002	8.64e-002	
North	-1.80e-002	9.40e-002	
Vertical	-3.48e-002	4.97e-002	

Positioning accuracy from 1:6500 imagery

- Differences at camera air stations obtained from 18 images (Mission D, 1:6500)
  Figure 8 Mission D

Statistical analysis [m]

Observation	RMS	Max.Dev.	at Image
East	3.03e-002	5.60e-002	161
North	6.60e-002	1.47e-001	165
Vertical	8.43e-002	1.39e-001	156
Observation	**Mean**	**Std.Dev.**	
East	6.26e-003	2.97e-002	
North	-3.56e-002	5.56e-002	
Vertical	7.74e-002	3.33e-002	

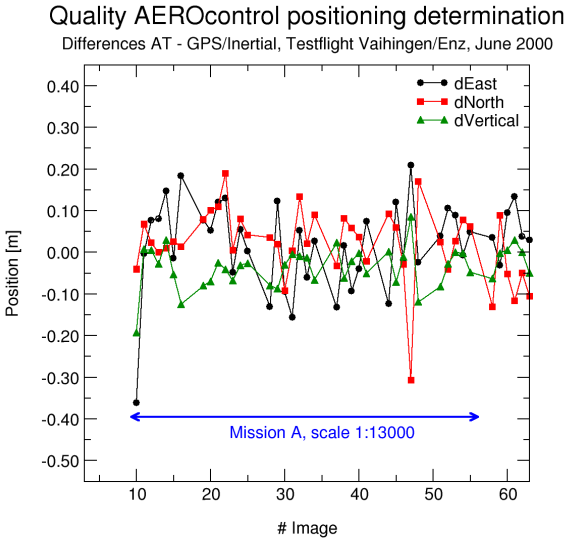

Figure 5, Position differences Mission A, 1:13000

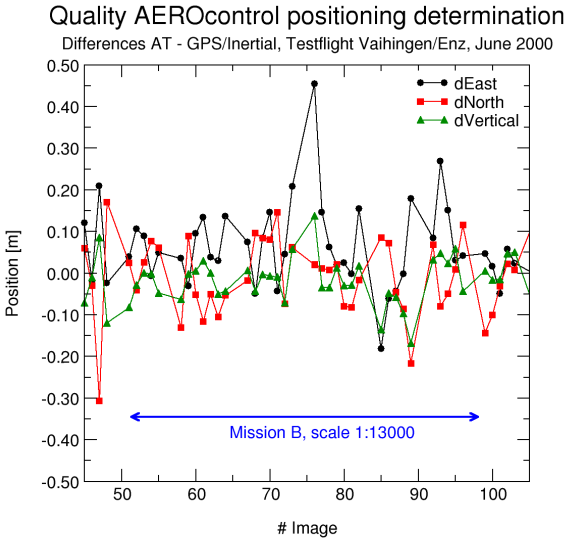

Figure 6, Position differences Mission B, 1:13000

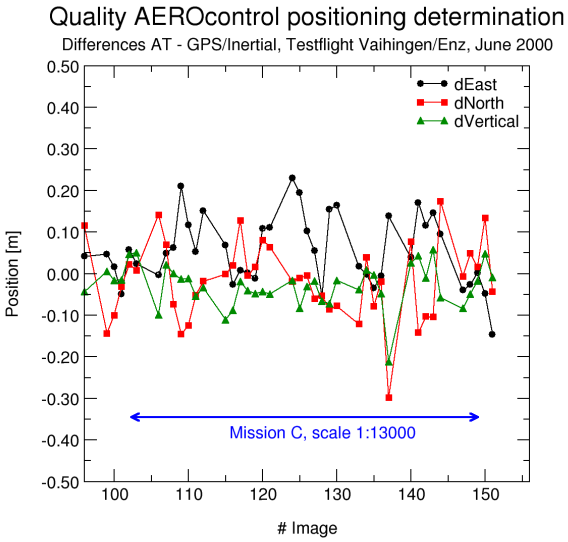

Figure 7, Position differences Mission C, 1:13000

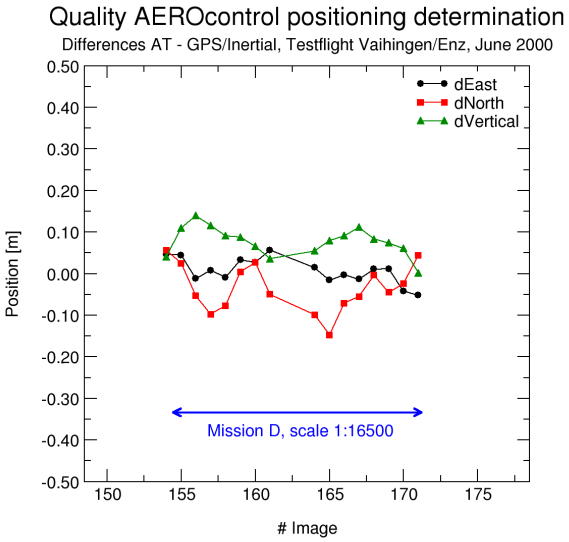

Figure 8, Position differences Mission D, 1:6500

Attitude accuracy from 1:13000 imagery

Boresight-Alignment obtained from 2 flight lines Mission A (lines #5, #6), 6 flight lines Mission B (lines #1-#6) and 1 flight line Mission C (line #1)

- Differences at camera air stations obtained from 3 x 36 images (Mission A, B, C, 1:13000)

  Statistical analysis [deg]

Observation	RMS	Max.Dev.	at Image
omega	2.67e-003	6.26e-003	29
phi	2.34e-003	7.74e-003	76
kappa	1.10e-002	3.89e-002	16
Observation	Mean	Std.Dev.	
omega	-2.83e-004	2.65e-003	
phi	6.40e-004	2.25e-003	
kappa	1.97e-003	1.09e-002	

- Differences at camera air stations obtained from 94 images (22 images Mission A (first two flight lines #1 and #2 excluded due to non optimal system alignment) and 2 x 36 images Mission B and Mission C)

  Statistical analysis [deg]

Observation	RMS	Max.Dev.	at Image
omega	2.53e-003	6.26e-003	29
phi	2.35e-003	7.74e-003	76
kappa	5.18e-003	1.20e-002	110
Observation	Mean	Std.Dev.	
omega	-7.18e-004	2.43e-003	
phi	5.21e-004	2.29e-003	
kappa	-1.25e-003	5.02e-003	

- Differences at camera air stations obtained from 36 images (Mission A, 1:13000)
  Figure 9 Mission A

  Statistical analysis [deg]

Observation	RMS	Max.Dev.	at Image
omega	2.99e-003	6.26e-003	29
phi	2.47e-003	6.39e-003	47
kappa	1.77e-002	3.89e-002	16
Observation	Mean	Std.Dev.	
omega	1.76e-003	2.41e-003	
phi	8.62e-005	2.47e-003	
kappa	8.79e-003	1.53e-002	

- Differences at camera air stations obtained from 36 images (Mission B, 1:13000)
  Figure 10 Mission B

  Statistical analysis [deg]

Observation	RMS	Max.Dev.	at Image
omega	1.86e-003	4.83e-003	64
phi	2.34e-003	7.74e-003	76
kappa	4.83e-003	1.09e-002	93
Observation	Mean	Std.Dev.	
omega	-2.33e-004	1.84e-003	
phi	1.21e-003	2.00e-003	
kappa	-1.90e-003	4.44e-003	

- Differences at camera air stations obtained from 36 images (Mission C, 1:13000)
  Figure 11 Mission C

Statistical analysis [deg]

Observation	RMS	Max.Dev.	at Image
omega	2.99e-003	6.13e-003	149
phi	2.19e-003	5.30e-003	119
kappa	5.68e-003	1.20e-002	110
Observation	Mean	Std.Dev.	
omega	-2.38e-003	1.81e-003	
phi	6.19e-004	2.10e-003	
kappa	-9.57e-004	5.60e-003	

Attitude accuracy from 1:6500 imagery

Same boresight alignment as in 1:13000 imagery used. Calibration angles obtained from 2 flight lines Mission A (lines #5, #6), 6 flight lines Mission B (lines #1-#6) and 1 flight line Mission C (line #1).

- Differences at camera air stations obtained from 18 images (Mission D, 1:6500)
  Figure 12 Mission C

Statistical analysis [deg]

Observation	RMS	Max.Dev.	at Image
omega	2.27e-003	3.19e-003	159
phi	1.81e-003	4.19e-003	165
kappa	6.70e-003	1.28e-002	161
Observation	Mean	Std.Dev.	
omega	-1.85e-003	1.31e-003	
phi	-2.66e-004	1.79e-003	
kappa	-4.49e-003	4.97e-003	

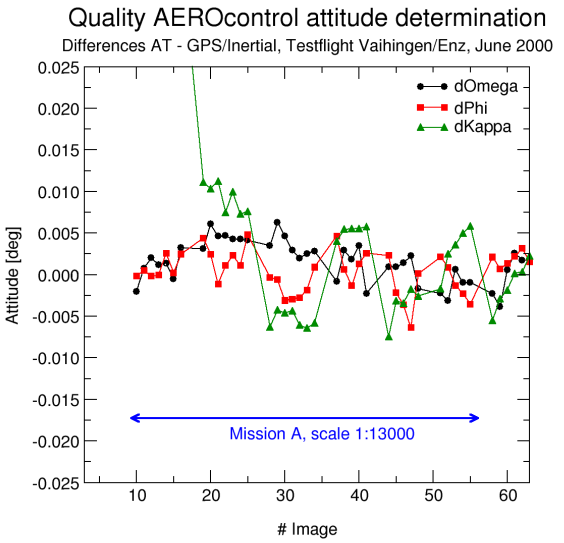

Figure 9, Attitude differences Mission A, 1:13000

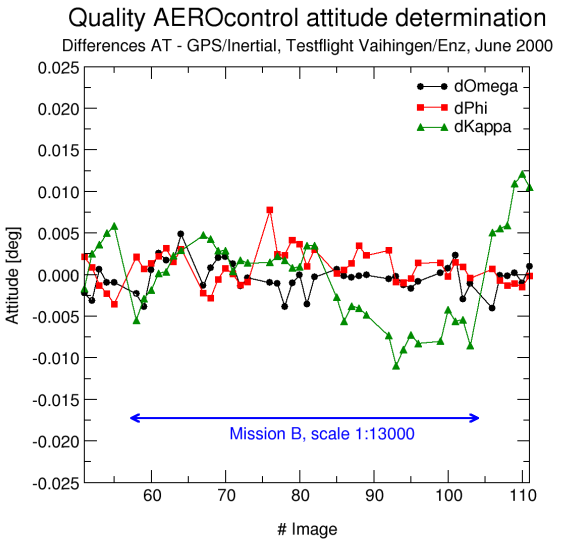

Figure 10, Attitude differences Mission B, 1:13000

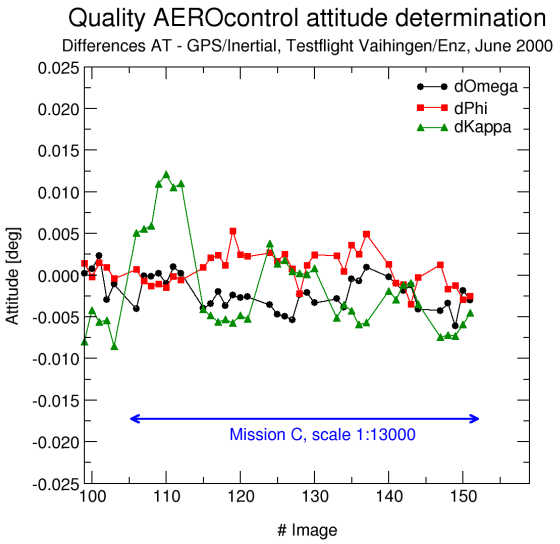

Figure 11, Attitude differences Mission C, 1:13000

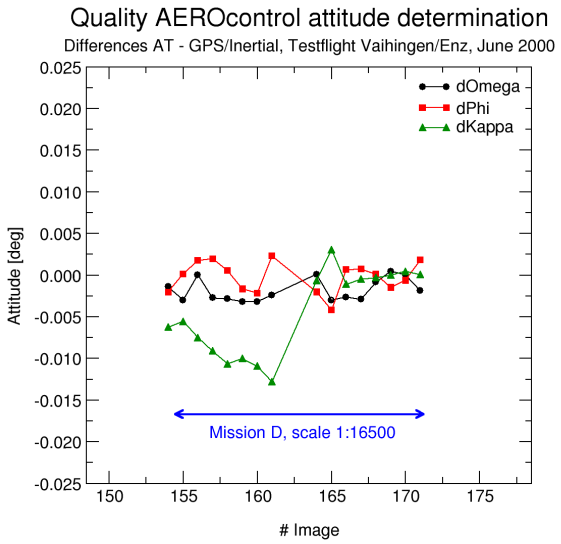

Figure 12, Attitude differences Mission D, 1:6500

Strip-wise analysis of attitude differences at camera air stations

Mission A,B,C: 1:13000, Mission D: 1:6500

Mission Line number	Δω [deg]		Δφ [deg]		Δκ [deg]	
	Mean	Std.Dev.	Mean	Std.Dev.	Mean	Std.Dev.
A, #1, 7 images	0.000830	0.001586	0.000749	0.001130	0.038062	0.000714
A, #2, 7 images	0.004437	0.000812	0.002136	0.001887	0.009280	0.001639
A, #3, 7 images	0.003506	0.001368	-0.001540	0.001423	-0.005411	0.000894
A, #4, 5 images	0.001006	0.002208	0.001535	0.001996	0.005249	0.000632
A, #5, 5 images	0.000750	0.001318	-0.001959	0.002997	-0.003690	0.001980
A, #6, 5 images	-0.001345	0.001298	-0.000838	0.002067	0.003032	0.002633
B, #1, 7 images	0.000731	0.002751	0.001994	0.000837	-0.000661	0.002734
B, #2, 7 images	0.000433	0.001390	-0.001005	0.001164	0.002580	0.001444
B, #3, 7 images	-0.001568	0.001411	0.003455	0.001989	0.002004	0.001034
B, #4, 5 images	-0.000040	0.000338	0.001546	0.001211	-0.004220	0.000983
B, #5, 5 images	-0.000904	0.000511	0.000374	0.001534	-0.008582	0.001356
B, #6, 5 images	-0.000167	0.001785	0.000618	0.000804	-0.006383	0.001644
C, #1, 7 images	-0.000584	0.001525	-0.000687	0.000688	0.008703	0.002839
C, #2, 7 images	-0.002989	0.000674	0.002342	0.001334	-0.005117	0.000514
C, #3, 7 images	-0.003780	0.001194	0.001275	0.001583	0.001180	0.001195
C, #4, 5 images	-0.001402	0.001731	0.002750	0.001480	-0.004942	0.000874
C, #5, 5 images	-0.001701	0.001323	-0.000943	0.001543	-0.002114	0.000969
C, #6, 5 images	-0.003747	0.001421	-0.001448	0.001467	-0.006510	0.001108
D, #1, 8 images	-0.002358	0.001049	0.000095	0.001733	-0.009111	0.002332
D, #2, 8 images	-0.001352	0.001351	-0.000629	0.001783	0.000114	0.001197
Mean of all lines	-0.000512	0.001352	0.000491	0.001532	0.000673	0.001435

Remarks on the quality of exterior orientations from IGI AEROcontrol system

The Figures 5-8 and the corresponding statistics show the typical results for this kind of investigation. Since the theoretical accuracy of the perspective centre coordinates from AT is dependent on image scale the values obtained from statistical analysis of the differences from large scale imagery are better compared to the 1:13000 imagery. Especially for the medium scale imagery the error of the independent values from AT plays a significant role in the difference – in other words, the values from AT could not be used as reference –, therefore only the results from the 1:6000 image blocks should be interpreted as GPS/inertial positioning accuracy. From these differences the obtained STD are well below 10cm which one could expect for airborne kinematic environments. Nevertheless, in the vertical and north coordinates small but significant offsets of ~8cm (vertical) and ~3cm (north) are visible. Such errors might be due to systematic errors in the positions from AT that are used for the comparison which underlines the problems using indirectly determined exterior orientations as references for the GPS/inertial quality investigation. As pointed out earlier the estimated orientations from AT are quite sensible on the used parameters in the adjustment and highly correlated. Uncorrected systematic errors are directly projected into the estimated orientation parameters. In this case, the vertical offset might be due to any scale dependent errors influencing the vertical component of the estimated camera stations. Most easily such offset can be explained by uncorrected influences of refraction or inconsistencies between the focal length from lab calibration – used in the bundle adjustment – and the true physical focal length during data acquisition. In contrary to these results no systematic height offset is present for the medium scale test blocks (Mission A,B,C). This can be interpreted as a sufficient agreement between the assumed parameters and the true physical environment conditions during data acquisition.

The performance of AEROcontrol attitude determination can be seen from Figures 9-12 for the medium and large scale image blocks, respectively. Except of the first two flight lines from Mission A where significant offsets in the kappa angle due to non optimal system alignment are clearly visible the remaining attitude differences are quite consistent. From the errors in kappa during the first two it has to be concluded that the well-known in-air alignment manoeuvre should be highly recommended even when there is only a quite short transition leg from the airport to the mission area. The RMS values are about 0.002 - 0.003deg for omega and phi-angle and about 0.005deg for kappa. The details can be read from the different statistical analysis. The high consistency shows, that the internal IMU sensor errors are damped quite effectively using the GPS update information. Analysing the attitude performance during single strips only, the quality of attitude determination is even more consistent. As listed in the table above, the mean STD from all 20 flight lines is about 0.0014deg for omega, phi and kappa.

Performance of direct georeferencing using exterior orientations from IGI AEROcontrol system

AEROoffice Software version 3.18
Exterior orientation elements provided from IGI at 17.01.2001

To assess the overall performance of the complete sensor system (AEROcontrol in combination with standard aerial camera RMK-Top), terrain coordinates of object points are re-determined by spatial intersection utilizing the corresponding image coordinates and the exterior orientations from direct georeferencing. This corresponds to a photogrammetric point determination, where aerial triangulation is replaced by direct georeferencing. The used image coordinates are only corrected by the influence of refraction, no correction of systematic errors are applied. In order to check the performance of direct georeferencing different versions using different block configurations and numbers of images are calculated. Calculating object coordinates using a large number of images results in a large number of image rays and in a higher redundancy for object point determination.

Direct georeferencing from 1:13000 imagery

- Analysis of check point residuals (Mission B, 1:13000)
  Statistics from 84 signalized points

  Statistical analysis [m]

Observation	RMS	Max.Dev.	at Point
East	5.48e-002	1.73e-001	10701
North	6.84e-002	1.80e-001	10102
Vertical	8.91e-002	2.64e-001	11002
Observation	Mean	Std.Dev.	
East	-6.57e-003	5.44e-002	
North	1.34e-002	6.71e-002	
Vertical	3.69e-002	8.11e-002	

- Analysis of check point residuals (Mission C, 1:13000)
  Statistics from 84 signalized points

  Statistical analysis [m]

Observation	RMS	Max.Dev.	at Point
East	7.13e-002	1.81e-001	10102
North	9.63e-002	3.01e-001	50102
Vertical	1.52e-001	3.76e-001	50401
Observation	Mean	Std.Dev.	
East	-1.82e-002	6.90e-002	
North	1.87e-002	9.44e-002	
Vertical	4.46e-002	1.45e-001	

- Analysis of check point residuals (Flight lines 1 and 3, Mission B, 1:13000, standard photogrammetric 60%, 20% overlap conditions)
  Statistics from 84 signalized points

  Statistical analysis [m]

Observation	RMS	Max.Dev.	at Point
East	5.59e-002	1.85e-001	10101
North	8.37e-002	2.32e-001	50102
Vertical	1.53e-001	4.83e-001	51001
Observation	Mean	Std.Dev.	
East	-1.25e-002	5.45e-002	
North	1.38e-002	8.26e-002	
Vertical	4.70e-002	1.46e-001	

- Analysis of check point residuals (Flight lines 1 and 3, Mission C, 1:13000, standard photogrammetric 60%, 20% overlap conditions)
  Statistics from 84 signalized points

  Statistical analysis [m]

Observation	RMS	Max.Dev.	at Point
East	1.13e-001	2.50e-001	31101
North	1.25e-001	2.84e-001	50102
Vertical	1.38e-001	3.82e-001	21301
Observation	Mean	Std.Dev.	
East	-7.54e-002	8.45e-002	
North	9.38e-002	8.38e-002	
Vertical	6.26e-002	1.23e-001	

- Analysis of check point residuals (Flight line 2, Mission B, 1:13000)
  Statistics from 49 signalized points

  Statistical analysis [m]

Observation	RMS	Max.Dev.	at Point
East	9.96e-002	2.12e-001	21201
North	6.60e-002	1.66e-001	41301
Vertical	1.80e-001	4.24e-001	41301
Observation	Mean	Std.Dev.	
East	7.76e-002	6.23e-002	
North	-2.12e-002	6.25e-002	
Vertical	9.30e-002	1.54e-001	

- Analysis of check point residuals (Flight line 3, Mission B, 1:13000)
  Statistics from 51 signalized points

  Statistical analysis [m]

Observation	RMS	Max.Dev.	at Point
East	5.20e-002	1.41e-001	30101
North	1.05e-001	2.32e-001	50102
Vertical	1.70e-001	4.83e-001	51001
Observation	Mean	Std.Dev.	
East	1.43e-002	4.99e-002	
North	5.76e-002	8.78e-002	
Vertical	8.39e-002	1.47e-001	

- Analysis of check point residuals (Flight line 2, Mission C, 1:13000)
  Statistics from 49 signalized points

  Statistical analysis [m]

Observation	RMS	Max.Dev.	at Point
East	9.90e-002	2.22e-001	41301
North	1.42e-001	2.92e-001	21301
Vertical	1.60e-001	3.54e-001	30102
Observation	Mean	Std.Dev.	
East	-3.26e-002	9.34e-002	
North	-1.21e-001	7.43e-002	
Vertical	4.54e-002	1.53e-001	

- Analysis of check point residuals (Flight line 3, Mission C, 1:13000)
  Statistics from 51 signalized points

  Statistical analysis [m]

Observation	RMS	Max.Dev.	at Point
East	8.37e-002	2.17e-001	50101
North	1.83e-001	3.11e-001	30201
Vertical	1.42e-001	2.94e-001	40201
Observation	Mean	Std.Dev.	
East	-7.53e-002	3.64e-002	
North	1.72e-001	6.44e-002	
Vertical	7.73e-002	1.19e-001	

Direct georeferencing from 1:6500 imagery

- Analysis of check point residuals (Mission D, 1:6500)
  Statistics from 30 signalized points

  Statistical analysis [m]

Observation	RMS	Max.Dev.	at Point
East	4.89e-002	1.39e-001	20901
North	6.42e-002	1.45e-001	11301
Vertical	8.66e-002	1.79e-001	51302
Observation	Mean	Std.Dev.	
East	1.32e-002	4.71e-002	
North	-1.83e-003	6.41e-002	
Vertical	-6.69e-002	5.50e-002	

- Analysis of check point residuals (Mission D, 1:6500)
  Statistics from 1465 automatically matched points from AAT

  Statistical analysis [m]

Observation	RMS	Max.Dev.	at Point
East	4.04e-002	1.46e-001	2000139
North	6.20e-002	1.71e-001	4000514
Vertical	8.95e-002	2.68e-001	4000514
Observation	Mean	Std.Dev.	
East	4.28e-003	4.02e-002	
North	2.58e-002	5.64e-002	
Vertical	-7.41e-002	5.01e-002	

- Analysis of check point residuals (Flight line 1, Mission D, 1:6500)
  Statistics from 21 signalized points

  Statistical analysis [m]

Observation	RMS	Max.Dev.	at Point
East	5.10e-002	1.00e-001	51302
North	8.86e-002	1.64e-001	31101
Vertical	8.33e-002	1.79e-001	51302
Observation	Mean	Std.Dev.	
East	3.74e-002	3.46e-002	
North	-3.19e-003	8.85e-002	
Vertical	-7.32e-002	3.96e-002	

- Analysis of check point residuals (Flight line 1, Mission D, 1:6500)
  Statistics from 843 automatically matched points from AAT

  Statistical analysis [m]

Observation	RMS	Max.Dev.	at Point
East	5.19e-002	1.75e-001	4000564
North	8.79e-002	2.19e-001	4000090
Vertical	8.73e-002	3.16e-001	4000329
Observation	Mean	Std.Dev.	
East	3.09e-002	4.17e-002	
North	2.65e-002	8.38e-002	
Vertical	-7.72e-002	4.07e-002	

- Analysis of check point residuals (Flight line 2, Mission D, 1:6500)
  Statistics from 15 signalized points

  Statistical analysis [m]

Observation	RMS	Max.Dev.	at Point
East	5.77e-002	1.39e-001	20901
North	3.44e-002	6.10e-002	21101
Vertical	7.57e-002	1.49e-001	20901
Observation	Mean	Std.Dev.	
East	-2.72e-002	5.09e-002	
North	3.12e-002	1.45e-002	
Vertical	-4.71e-002	5.92e-002	

- Analysis of check point residuals (Flight line 2, Mission D, 1:6500)
  Statistics from 885 automatically matched points from AAT

  Statistical analysis [m]

Observation	RMS	Max.Dev.	at Point
East	4.89e-002	1.67e-001	4000511
North	4.14e-002	1.12e-001	4000231
Vertical	8.84e-002	3.10e-001	4000408
Observation	Mean	Std.Dev.	
East	-1.79e-002	4.55e-002	
North	3.58e-002	2.09e-002	
Vertical	-6.36e-002	6.15e-002	

Main results of direct georeferencing

Performance (RMS, maximum deviation) using different block configurations (extract from the results given in the detailed statistics above):

- Cross flight pattern, high overlap, up to 16-folded points: Mission B, 1-6, Mission C, 1-6
- Standard photogrammetric overlap, up to 6-folded points: Mission B, 1+3, Mission C, 1+3, Mission D, 1+2
- Single flight lines, 3-folded points maximum: Mission B, 2, Mission B, 3, Mission C, 2, Mission C, 3, Mission D, 1, Mission D, 2

Version	East [cm]		North [cm]		Vertical [cm]	
Line number	RMS	Max.Dev.	RMS	Max.Dev.	RMS	Max.Dev.
Mission B, 1-6	5.5	17.3	6.8	18.0	8.9	26.4
Mission C, 1-6	7.1	18.1	9.6	30.1	15.2	37.6
Mission B, 1+3	5.6	18.5	8.4	23.2	15.4	48.3
Mission C, 1+3	11.3	25.0	12.6	28.4	13.8	38.2
Mission D, 1+2	4.9	13.9	6.4	14.5	8.7	17.9
Mission B, 2	10.0	21.2	6.6	16.6	18.1	42.4
Mission B, 3	5.2	14.1	10.5	23.2	17.0	48.3
Mission C, 2	9.9	22.2	14.2	29.2	16.1	35.4
Mission C, 3	8.4	21.7	18.4	31.1	14.2	29.4
Mission D, 1	5.1	10.0	8.8	16.4	8.3	17.9
Mission D, 2	5.7	13.9	3.5	6.1	7.6	14.9

Remarks on the quality of direct georeferencing from IGI AEROcontrol system

The quality of direct georeferencing using AEROcontrol exterior orientations is very satisfying and almost in the range of the accuracy potential from standard aerial triangulation. As it can be seen from the table and the detailed statistics above, RMS values of about 5-15cm and 8-18cm are possible for the horizontal and vertical object coordinates, respectively. In general, the use of multiple images providing strong overlap conditions is preferable for higher accuracy on the ground. Nevertheless, even the direct georeferencing of single flight lines which is somehow critical from photogrammetric point of view obtains sufficient accuracy. Using large scale imagery from lower altitudes results in slightly better object point quality.

Concluding remarks

This empirical test has shown the high potential of the AEROcontrol system. Based on this specific performance investigation the directly determined exterior orientation parameters from AEROcontrol are obtained with an accuracy of ~5-10cm (RMS) for position and 0.002-0.003deg (RMS) for omega and phi and 0.005-0.007deg (RMS) for kappa angle. Using the GPS/inertial exterior orientations direct georeferencing of standard analogue photogrammetric cameras is possible with an accuracy (RMS) of 5-15cm for the horizontal and 8-18cm for the vertical coordinates. This accuracy is obtained without any ground control. Since the test flight is well controlled the obtained results are representative and should be reproducible in a production environment under optimal conditions. Nevertheless, the quality has to be verified in future tests and true production environments, where e.g. the calibration site for system calibration is totally different from the mission area.

In general, the overall system calibration is the most demanding task in direct georeferencing. Therefore future work has to be focussed on this topic. From a practical point of view optimal calibration procedures have to be defined. Especially for the boresight alignment the exterior orientations from AT are essential and recommendations for an optimal design for the calibration block are necessary. Additionally the stability of system calibration over longer time periods and the quality of the calibration transfer from the calibration site to the mission area has to be investigated.

Finally, as one major point, aspects on reliability have to be considered. The system reliability is very important for example for orthoimage production where digital terrain models are available. Using direct georeferencing for such applications the requirements on standard photogrammetric image overlap can be reduced to an absolutely minimum to minimize flying time and number of imagery. Since this scenario relies on the GPS/inertial exterior orientations totally, undetected errors in the integrated system would prevent the successful image evaluation. Therefore the quality of the different hardware components has to be checked permanently, preferable during data acquisition using the real-time capability of Kalman filtering to allow fast interaction. If possible, a redundant data acquisition should be aspired, at least for the GPS reference stations. With multiple reference stations a multi-station GPS processing will be possible which will increase the accuracy and reliability of GPS data as the main update information and will influence the resulting integrated system performance. From this point of view the use of centralized or adaptive Kalman filtering is very promising.

To conclude, the following final remarks should be mentioned:

- Direct georeferencing is an excellent tool for fast and flexible sensor orientation.
- The GPS/inertial technology is mature for the practical use.
- Integrated GPS/inertial systems will become a standard tool for airborne sensor orientation. The acceptance of this technology will be pushed by the growing distribution of the new digital airborne sensors.